Carbohydrate Polymers 103 (2014) 310–318

Contents lists available at ScienceDirect

Carbohydrate Polymers

journal homepage: www.elsevier.com/locate/carbpol

Preparation and characterization of starch crosslinked with sodium trimetaphosphate and hydrolyzed by enzymes

Fei Gao[a], Dong Li[a,*], Chong-hao Bi[a], Zhi-huai Mao[a], Benu Adhikari[b]

[a] College of Engineering, National Energy R&D Center for Non-food Biomass, China Agricultural University, PO Box 50, 17 Qinghua Donglu, Beijing 100083, China

[b] School of Applied Sciences, RMIT University, City Campus, Melbourne, VIC 3001, Australia

ARTICLE INFO

Article history:
Received 4 July 2013
Received in revised form 5 November 2013
Accepted 10 December 2013
Available online 17 December 2013

Keywords:
Porous starch
Cross-linking
Swelling
Adsorption kinetics
Viscosity

ABSTRACT

Crosslinked porous starch samples were produced by first crosslinking corn starch with sodium trimetaphosphate (STMP) and then partially hydrolyzing it with a mixture of α-amylase and glucoamylase. The granule morphology, porosity, swelling power, adsorption capacity, crystalline nature, molecular structure, melting and viscometric properties of these starch samples were measured and analyzed. The results showed that the porous starch which was crosslinked with 6% (w/w) STMP (ScPS-6) possessed remarkable superiority in terms of thermal and shear resistance among all the starch samples tested. The ScPS-6 also had the highest porosity and largest average pore diameter values. The swelling power of crosslinked porous starch was 56.3% lower than that of uncrosslinked porous starch. First order reaction kinetics equation was found to excellently ($R^2 \geq 0.99$, average error = 6.03%) predict the experimental adsorption kinetics data of methylene blue for the crosslinked porous starch samples.

1. Introduction

Starch is an abundant, biodegradable and renewable biopolymer which is immensely important as food as well as industrial ingredient (Szabo-Revesz, Szepes, Ulrich, Farkas, & Kovacs, 2007). Starch contributes greatly to the textural properties of many food products and it is commonly used in food and other industrial applications as a thickener, a stabilizer, a gelling agent, a bulking agent and water retaining agent (Svegmark & Hermansson, 1993; Singh, Kaur, & McCarthy, 2007). However, starch has intrinsic disadvantages such as very weak resistance against shear and heat, very high susceptibility to thermal decomposition and high tendency to undergo retrogradation (Singh et al., 2007; Jobling, 2004; Raina, Singh, Bawa, & Saxena, 2007; Peng et al., 2011a,b; Yan & Zhengbiao, 2012). Starch has the potential for much greater application in food and other industries if the above mentioned intrinsic disadvantages are technologically overcome. The physical and chemical characteristics of starch can be modified to overcome its inherent limitations and to improve its functionality (Chen, Zhang, & Chen, 2011; Chen, Huang, Tang, Chen, & Zhang, 2011; Hermansson & Svegmark, 1996).

The modification of starch can be carried out by using a number of physical and chemical methods or the judicious combination of these methods. Physical modification is achieved by using hydrothermal processing (gelatinization). The chemical treatments involve the introduction of suitable functional groups into the starch molecule using derivatization reactions such as etherification, esterification, crosslinking and grafting or decomposition reactions such as acid or enzymatic hydrolysis and oxidation (Loacutepez, Zaritzky, & Garciacutea, 2010; Wurzburg, 1986; Singh et al., 2007). Chemical modification is commonly used for improving the properties of starch in order to meet the requirements of specific applications (Han & BeMiller, 2008). One of the most commonly used ways to modify starch is the crosslinking, which is intended to add intra- and inter-molecular bonds at random locations of a starch molecule (Acquarone & Rao, 2003). Sodium trimetaphosphate (STMP), sodium tripolyphosphate (STPP), epichlorohydrin (EPCH), phosphoryl chloride ($POCl_3$), a mixture of adipic acid and acetic anhydride, and vinyl chloride are some of the common crosslinking agents currently used to crosslink with starch (Wattanchant, Muhammad, Hashim, & Rahman, 2003; Woo & Seib, 1997; Wu & Seib, 1990; Yook, Pek, & Park, 1993). Epichlorohydrin (EPCH) has been reported as a common crosslinker used to modify starch (Yu & Liu, 1994; Hamdi, Ponchel, & Duchêne, 1998; Atyabi, Manoochehri, Moghadam, & Dinarvand, 2006; Zhou et al., 2006). However, EPCH is known to be toxic and the presence of small quantity of its residue or unreacted fraction can lead to toxic side effects (Li et al., 2009). More recently, sodium trimetaphosphate (STMP) has been proposed as a non-toxic crosslinker of starch (Li et al., 2009) because it does not

* Corresponding author. Tel.: +86 10 62737351; fax: +86 10 62737351.
E-mail address: dongli@cau.edu.cn (D. Li).

0144-8617/$ – see front matter © 2013 Elsevier Ltd. All rights reserved.
http://dx.doi.org/10.1016/j.carbpol.2013.12.028

have adverse effects on humans (Woo & Seib, 1997). Because of this reason we have selected STMP as a crosslinker of starch. STMP is reported to efficiently crosslink with semidry starch at high temperature (60–70 °C) (Kerr & Cleveland, 1962). STMP is also reported to efficiently crosslink with hydrated starch in starch slurry at moderately high temperature (40–45 °C) (Singh et al., 2007).

Porous starch (PS) is a versatile, cheaper and biodegradable adsorbent containing large number of micron-sized pores. It has been widely used in food, pharmaceutical, agriculture, cosmetics, pulp and paper industries (Qian, Chang, & Ma, 2011). Earlier investigations have shown that enzymatic hydrolysis is a better method in preparing porous starch (Zhang et al., 2012; Chen et al., 2011; Wu, Du, Ge, & Lv, 2011; Uthumporn, Zaidul, & Karim, 2010). However, the enzymatic hydrolysis, if the process is not properly designed, can easily destroy the granular structure of porous starch. When the granular structure is destroyed, some physical properties such as gelatinization temperature, freeze-thaw stability, tackiness and the stability against shear are negatively impacted. In order to maintain the physical properties of crosslinked starch superior to those of native starch, a proper selection of crossliker and crosslinking method is essential.

In this study, starch was crosslinked by sodium trimetaphosphate (STMP) followed by partial enzymatic hydrolysis of starch using a mixed enzyme system. The crosslinked porous starch samples were examined using a scanning electron microscope to observe the change in the starch granules. The effect of crosslinking on the molecular structure of starch was assessed by using FTIR. The thermal properties such as glass transition and melting temperatures of the crosslinked porous starch granules were determined using a DSC. The uncrosslinked porous starch and native starch samples were also investigated along with the crosslinked porous starch for comparison purpose.

2. Materials and methods

2.1. Materials

Corn starch was obtained from Yujing Food Co. Ltd (Henan, China). Sodium trimetaphosphate (STMP) was purchased from Beijing Chemical Company (Beijing, China). α-Amylase (activity = 3.7 unites/mg) and glucoamylase (activity = 100 unites/mg) were purchased from Aoboxing Biological Technology Co. Ltd. (Beijing, China). The methylene blue was provided by Jinke Chemical Industry Research Institute (Tianjin, China). All of these reagents were of analytical grade and were used without further purification. Deionized water was used throughout the work.

2.2. Preparation of STMP-crosslinked starch

STMP-crosslinked starch samples were prepared using STMP as crosslinker according to the method of Mao, Wang, Meng, Zhang, and Zheng (2006). Corn starch (50 g) was added into 100 mL distilled water which contained 1 g Na_2CO_3 (2 g/100 g dry starch) and 2.5 g NaCl (5 g/100 g dry starch). The crosslinking agent (STMP), was dissolved in the starch containing slurry varying its amount from 1 g to 4 g to form four samples having four different crosslinking degrees (2%, 4%, 6%, and 8%, w/w). Then, the mixture was stirred using a magnetic stirrer at 200 rpm for 80 min at 50 °C in a thermostated water bath. Hydrochloric acid (1 M) was used to adjust the pH of slurry to 6.5. After the solid portion was precipitated, the supernatant was discarded and the solid portion was washed with deionized water. In this way crosslinked starch samples having different degree of crosslinking were obtained. The crosslinking reaction involved in the STMP-starch crosslinking is given below (Liu, 2001).

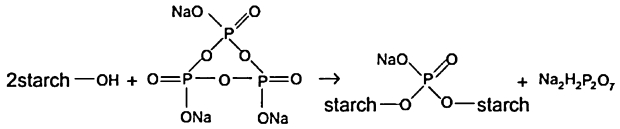

2.3. Preparation of STMP-crosslinked porous starch (ScPS)

Starch slurry (25% w/v) containing the crosslinked starch (described in Section 2.2 above) was prepared using 200 mL of sodium acetate buffer (pH = 4.6). This slurry was stirred for 20 min at 150 rpm in a water bath maintained at 40 °C as proposed by Whistler (1991). After preheating the slurry for 20 min, a mixture of α-amylase and glucoamylase at the ratio (α-amylase to glucoamylase) of 1:4 was added into the slurry. The enzyme to starch ratio was 1:100 (w/w). The slurry samples were then stirred using a magnetic stirrer at 150 rpm for 14 h while maintaining the temperature at 40 °C. Upon completion of the enzymatic reaction (14 h), the enzymes were inactivated and the hydrolysis was stopped by adding 20 mL of NaOH solution (4%, w/w). The resultant hydrolyzed starch suspension was centrifuged at 1007.1*g* for 5 min. The starch product obtained by centrifugation was washed three times in order to remove the non-starch components (Zhang et al., 2012; Chang, Yu, & Ma, 2011). Finally, the washed product was collected and dried using a vacuum freeze dryer (LGJ-18C, Four-Ring Science Instruments Plant Co. Ltd., Beijing, China). The starch product was first frozen at −30 °C for 1 h and then it was dried in the vacuum chamber by maintaining the pressure at 1.0 Pa. The heating rate within the dryer was maintained at 5 °C/h until the temperature reached 25 °C. The total drying time was 12 h.

2.4. Examination of morphology

The morphology of starch granules was observed using a scanning electron microscope (S-3400N, Hitachi Instruments Ltd., Japan). The sample particles were evenly distributed on SEM specimen stubs with double-sided adhesive tape, and sputtered with gold. The shape and the surface characteristics of the sample particles were observed and analyzed at an operating voltage of 15 kV.

2.5. Porosity test

The porosity of samples was measured using an automatic mercury porosimeter (AutoPore IV 9510, micromeritics Inc., America). Starch samples (1 g) were dried at 105 °C, placed in a dilatometer attached with the porosimeter and then out-gassed under high vacuum. The pores of the out-gassed samples were filled with mercury under the pressure varying from 0.0036 MPa to 413 MPa. Mean pore radius (r) was calculated according to Eq. (1) based on the assumption of cylindrical pores. Five replicate tests were made to determine the average diameter for each ample.

$$R = \frac{(2 \times \gamma/\cos\theta)}{p} \quad (1)$$

where γ is the surface tension of mercury (0.48 J/m^2), θ is the contact angle (140°) and p is the applied pressure (MPa).

2.6. Degree of swelling

The degree of swelling was determined using a mass gain method reported by Lin, Yu, and Yang (2005) with some modification. Briefly, 2.5 g of porous starch samples (having different degree of crosslinking) were added into 50 mL of deionized water and heated at 45 °C, 70 °C, 90 °C for 5 h. Then, these samples were centrifuged at 11,190*g* for 10 min. The surface water of the centrifuged starch samples was removed by using blotting paper and

then the mass was measured immediately. The degree of swelling was calculated according to Eq. (2).

$$\text{degree of swelling}\,(\%) = \frac{W_s - W_d}{W_d} \quad (2)$$

where W_s is the mass (g) of crosslinked porous starch in swollen state while W_d is the dry mass (g) of crosslinked porous starch.

2.7. Methylene blue adsorption test

The freeze dried crosslinked porous starch (2.0 g) was added to 50 mL methylene blue solution (0.02 g/L) and stirred for 5 h using a magnetic stirrer. Then, the suspension was centrifuged at 11,190*g* for 10 min. The amount of unadsorbed methylene blue remaining in the supernatant was measured by the absorbance of the supernatant at 665 nm using ultraviolet/visible spectrophotometer (TU-1810, Purkinje General Instrument Co. Ltd., Beijing, China).

The adsorption ratio was calculated using Eq. (3), given below.

$$\text{adsorption ratio}\,(\%) = \frac{C_0 - C_1}{C_0} \quad (3)$$

where C_0 is concentration (g/L) of methylene blue in solution before adsorption. C_1 is residual concentration (g/L) of methylene blue in the supernatant after adsorption. In this study, the value of C_0 was 0.02 g/L.

2.8. X-ray diffraction (XRD)

The XRD diffractograms of the native corn starch and the crosslinked porous starch were obtained using a X-ray diffractometer (MSAL-XD2, Purkinje general instrument Co. Ltd., Beijing, China).These samples were scanned in the angular range of 10–40° (2θ) with a scanning rate of 1°/min and sampling interval of 0.02°. X-ray powder diffraction analysis was then performed at 36 kV and 20 mA using nickel-filtered Cu $K\alpha$ ($\lambda = 1.5406$ Å) radiation. The diffracted radiation was detected using a proportional detector.

2.9. Fourier transform infrared spectroscopy (FT-IR)

The FT-IR experiments were performed by using a FTIR spectrometer (Spectrum RX/BX series, Perkin Elmer, USA). The spectra of the crosslinked porous starch were acquired and compared with the spectra of the uncrosslinked (blank) porous starch. Tablets comprising KBr (200 mg) and crosslinked porous starch (2 mg) were used in FTIR tests. The samples for the blank tests were prepared in the identical manner. Scanning was performed from 4000 cm^{-1} to 400 cm^{-1} at a resolution of 4 cm^{-1}. The interference of water vapor and CO_2 from air on the FTIR spectra was deducted during scanning.

2.10. Measurement of glass transition temperature (T_g)

A DSC (Q10, TA Instrument, USA) was used to measure the glass transition temperature (T_g) of the crosslinked porous starch. Powder samples of 4–6 mg were weighed in aluminum pans and hermetically sealed. The thermal analyses were performed within a temperature range of −40 °C to 200 °C. A heating rate of 10 °C/min was used throughout these thermal scans using nitrogen as the flushing gas.

2.11. Measurement of viscosity

The viscosity of native and the crosslinked porous starches was measured using a rheometer (AR2000ex, TA Instruments Ltd., Crawley, UK). An aluminum parallel plate (40 mm diameter, 1 mm gap) was chosen for this purpose. A thin layer of low viscosity silicon oil was applied on the surface of the samples in order to prevent evaporation. Two grams of dried starch sample was dispersed in 25 mL distilled water and shaken for 1 min before the slurry was loaded to the measuring plate. The slurry was first heated to 50 °C and it was held at this temperature for 1 min. Subsequently, the temperature of the sample was increased to 95 °C in 10 min and it was held at this temperature for 5 min. After the completion of this heating cycle, the dispersion was cooled to 50 °C in 7 min and it was held at this temperature for 5 min. All experiments were conducted at a shear rate of 200 1/s. The data were collected in 10 s interval.

The relevant parameters such as peak viscosity, holding strength, final viscosity, breakdown, and setback were determined according to the definition provided by Wongsagonsup, Shobsngob, Oonkhanond, and Varavinit (2005).

- Peak viscosity is the highest viscosity during the heating step.
- Holding strength is the lowest viscosity at the end of the 95 °C heating step.
- Final viscosity is the viscosity at the end of 50 °C cooling step.
- Breakdown is the ratio of peak viscosity to holding strength.
- Setback is the change in viscosity from holding strength to final viscosity.

2.12. Statistical analysis

All the above mentioned tests were carried out in triplicate and the results are expressed as the mean ± standard deviation. Duncan's multiple comparison tests were used to determine the significant difference between mean values at 95% ($p < 0.05$) confidence level using SPSS 19.0 software (SPSS Inc., Chicago, USA).

3. Results and discussion

3.1. Morphology of starch granules

The morphology of native starch, STMP-crosslinked starch and STMP-crosslinked porous starch (ScPS) as observed under SEM are presented in Fig. 1. As can be seen from the SEM micrograph (Fig. 1, label NS), the native starch granules have round and polygonal granular shape with relatively smooth surface which agrees with earlier observations by Zhang et al. (2012). The granules of the STMP-crosslinked starch (CL) appear rougher and they have some surface dents.

The SEM micrographs of STMP-crosslinked porous starch having different degree of crosslinking (2%, ScPS-2; 4%, ScPS-4; 6%, ScPS-6; 8%, ScPS-8) are presented in Fig. 1. It can be seen from the SEM micrographs of crosslinked porous starch samples that there are a large number of pores on the surface of porous starch granules. O'Brien and Wang (2008) have also reported that larger and deeper pore structures are formed during enzymatic hydrolysis of starch granules due to extensive enzymatic hydrolysis. However, the number and the size of pores in porous starch having different degree of crosslinking are different. Especially, the morphology of ScPS-4 is quite different compared to others. The size of pores in the ScPS-4 is the smallest and the number of pores in this sample was the highest compared to other three crosslinked porous starch samples. The pores in the ScPS-2 are relatively shallow. This may be due to the fact that degree of crosslinking (2%) at this level does not facilitate the enzymatic hydrolysis. The size and shape of pores in ScPS-6 are similar to those in ScPS-2 and ScPS-8. The depth of pores in ScPS-6 has increased compared to that of ScPS-2 and as would be shown in Section 3.2 below, this sample showed the highest porosity. It can also be seen from this figure that some of the pores of ScPS-8 have merged (collapsed) with each other.

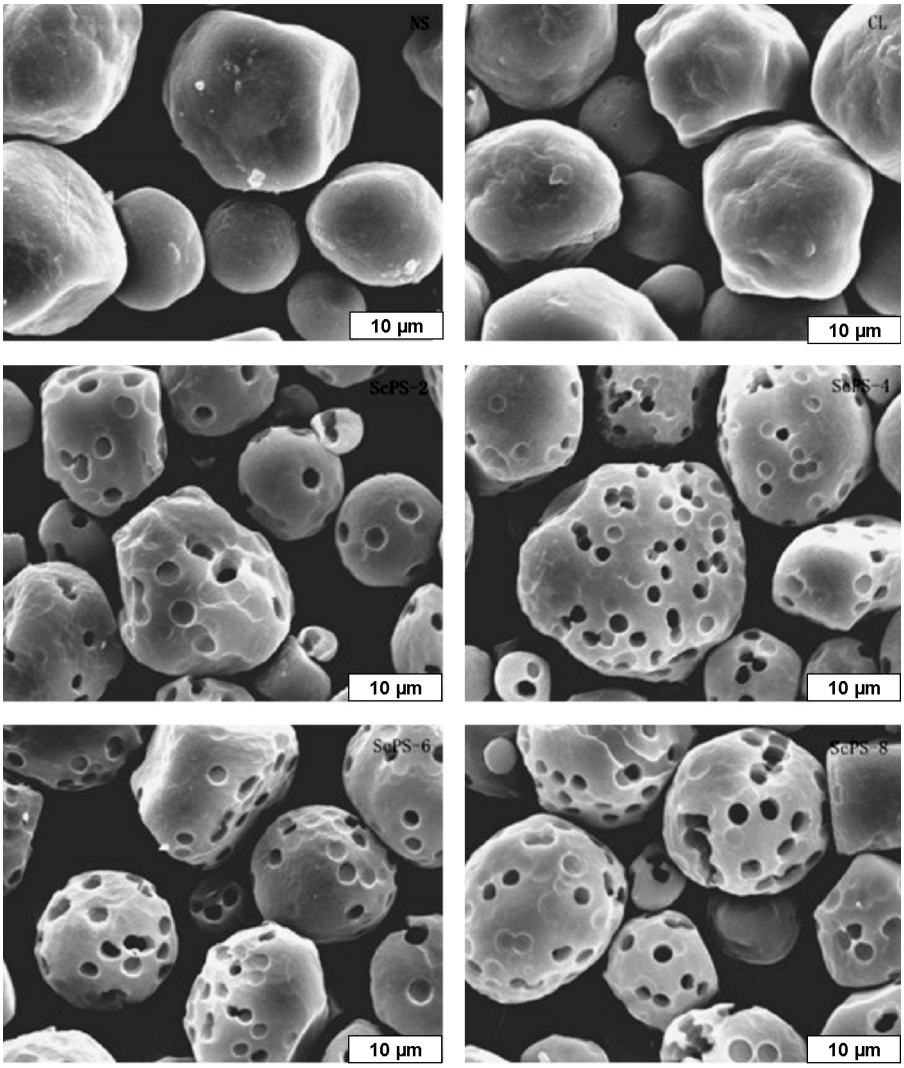

Fig. 1. SEM micrographs of native starch (NS), crosslinked starch (CL) and crosslinked porous starch (ScPS-2, ScPS-4, ScPS-6, ScPS-8).

The increase in pore size and pore depth in the structure of crosslinked porous starch compared to that of native search indicates that the former is capable of offering larger specific surface area (Chen & Zhang, 2012). It can be inferred from the highly porous structure of crosslinked porous starch granules that this starch would have higher adsorption capacity compared to native starch. Hence, the crosslinked porous starch can be preferably used as an adsorbent in various applications.

3.2. Porosity of starch samples

Table 1 presents the data on total pore area, average pore diameter and porosity of native starch and porous starch with different crosslinking degree. The hydrolysis caused an obvious increase in pore area and pore diameter as well as the porosity. The magnitude of the total pore area of crosslinked porous starch was increased 10–20 times compared to that of the native starch. The ScPS-6 and ScPS-8 have relatively higher total pore area. This may be due to the fact that these two samples possess relatively higher porous structure with higher degree of STMP crosslinking. The average pore diameters of native and STMP-crosslinked porous starches (Table 1) show the latter have significantly ($p < 0.05$) larger pore diameters which corroborate with the corresponding morphological features (Section 3.1). The STMP-crosslinked porous starch possess significantly ($p < 0.05$) higher porosity than that of native starch (Table 1). The ScPS-6 shows the highest porosity value among all the samples. These observations indicate that the surface of the crosslinked porous starch contains much higher number of pores and that the degree of crosslinking affects the porosity of the porous starch. These observations also corroborate with the morphological features (Section 3.1) that the enzymatic hydrolysis has produced

Table 1
Total pore area, average pore diameter and porosity for native starch (NS) and crosslinked porous starch (ScPS) samples.

Starch species	Total pore area (m^2/g)	Average pore diameter (4 V/A) (nm)	Porosity (%)
NS	0.394 ± 0.02^a	26.9 ± 1.4^a	7.13 ± 0.3^a
ScPS-2	1.632 ± 0.06^b	1052.4 ± 33^c	53.92 ± 0.18^b
ScPS-4	4.237 ± 0.15^c	$969.8 \pm 19^{b,c}$	59.73 ± 0.21^c
ScPS-6	7.045 ± 0.34^d	1506.4 ± 28^d	62.86 ± 0.26^d
ScPS-8	6.807 ± 0.26^d	790.9 ± 32^b	$57.97 \pm 0.32^{b,c}$

ScPS-2, 4, 6, and 8 denote 2%, 4%, 6% and 8% of crosslinking in porous starch samples.
Values represent the mean ± standard deviation of triplicate tests.
Values in a column followed by different lowercase letters in superscripts were significantly different from each other according to Duncan's multiple range tests ($p < 0.05$).

Table 2
The degree of swelling (%) of native starch (NS), porous starch (PS) and crosslinked porous starch (ScPS) samples.

Samples	40 °C	70 °C	95 °C
NS	4.9216 ± 0.24^{a}	15.4529 ± 0.76^{e}	43.9021 ± 0.48^{a}
PS	6.5374 ± 0.61^{d}	17.3532 ± 0.15^{f}	48.1736 ± 0.81^{d}
ScPS-2	6.4917 ± 0.33^{d}	$14.8786 \pm 0.59^{b,c}$	45.8336 ± 0.27^{b}
ScPS-4	6.1337 ± 0.47^{c}	$14.6962 \pm 0.75^{a,b}$	44.0718 ± 0.37^{a}
ScPS-6	6.0345 ± 0.13^{c}	14.5774 ± 0.55^{a}	46.8598 ± 0.86^{c}
ScPS-8	5.6914 ± 0.29^{b}	15.2911 ± 0.72^{d}	46.9264 ± 0.64^{c}

ScPS-2, 4, 6, and 8 denote 2%, 4%, 6% and 8% of crosslinking in porous starch samples.
Values represent the mean ± standard deviation of triplicate tests.
Values in a column followed by different lowercase letters in superscripts were significantly different from each other according to Duncan's multiple range tests ($p < 0.05$).

starch granules with much higher porosity (more porous granule structure). Furthermore, the porous starch with 6% crosslinking degree showed the highest values in total pore area, average pore diameter and porosity.

3.3. The degree of swelling

Table 2 shows the degree of swelling of STMP-crosslinked porous starch (ScPS) samples prepared at different level of STMP concentration. It be seen from this table that the degree of swelling (swelling power) of ScPS has increased significantly ($p < 0.05$) with the increase in the temperature. This observation indicates that temperature is the important factor which affects the swelling power of crosslinked porous starch.

Table 2 showed that the degree of swelling of porous starch is higher than that of native starch. This can be attributed to the large number of pores in the partially hydrolyzed starch granules (Section 3.2) possess large number of pores. The increase in the number and size of the pores can hold more water within the starch granules which results into higher swelling power. In addition, the amylose content (amorphous region) of starch is degraded in the hydrolysis process. It has been reported earlier that the starch granules containing lower extent of amylose swell more easily when subjected to heat (Wang & Wang, 2003). The degree of swelling of crosslinked porous starch was lower than that of porous starch. This may be due to the crosslinking of starch molecules with STMP increases and strengthens strength of hydrogen bonds. The increased strength of hydrogen bonds can restrict the swelling power of STMP crosslinked porous starch (Lee et al., 2000).

The swelling power of crosslinked porous starch at different temperature was different depending on the degree of crosslinking. For example, the degree of swelling of ScPS-2 was the highest and that of ScPS-8 was the lowest at 40 °C. This is consistent with Lee, Kumar, Rozman, and Azemi's (2005) report that the strength of bonding of the starch granules plays an important role in determining the extent to which the starch granules are capable of swelling. Hence the degree of swelling of the crosslinked starch at 40 °C is expected to be controlled by the concentration of the crosslinker. This is because starch is well below its gelatinization temperature.

The degree of swelling at 70 °C is quite different compared to the degree of swelling at 40 °C. That is, the swelling power of the crosslinked porous starch decreased with the increase in the STMP concentration. The swelling power of the crosslinked starch reached to its minimum value at 6% STMP concentration. The swelling power of the crosslinked starch at 8% STMP was higher than that at 6% HTMP. This trend of variation of swelling power of crosslinked starch can be attributed to the increase in the density of crosslinks. This increased crosslinking density hinders the penetration of water into the starch molecular network and results into the reduction of swelling power. Hirsch and Kokini (2002) showed

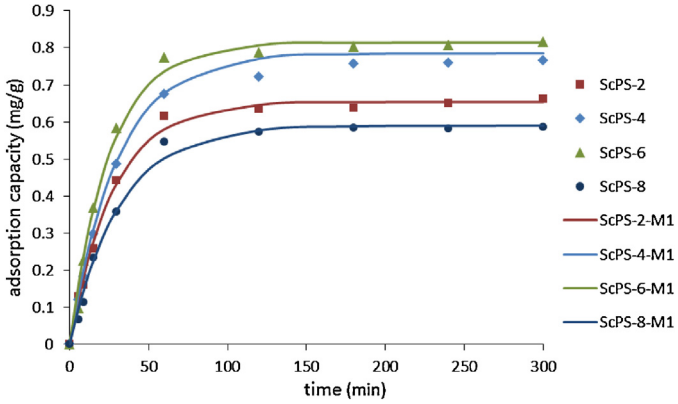

Fig. 2. Adsorption kinetics of methylene blue (MB) in porous starch samples at different crosslinking degree.

that the crosslinked starch became stiffer and the starch granule became more compact when the degree of crosslinking increased. In another study, De Miguel, Rieumajou, & Betbeder (1999) found that at very high concentration of epichlorohydrin, the crosslinker was found to polymerise to form longer poly-oxyethylene-type crosslinks between the polymer chains. The resultant dimeric or oligomeric structures were found to facilitate the swelling rather than restricting it. This observation helps to explain why the swelling power of ScPS-8 was higher than that of ScPS-6.

At 95 °C, the variation of the degree of swelling of all the starch samples was similar. The degree of swelling of all the samples was highest at this temperature compared to the degree of swelling at lower temperatures. This is due to the fact that the starch samples were sufficiently gelatinized during the hydrothermal processing and the amylopectin chains were hydrolyzed at this high temperature. Furthermore, we found the water content of the swelled starch could not completely be separated by centrifugation (Wang & Wang, 2003).

3.4. Adsorption kinetics

Fig. 2 presents the adsorption capacity (for methylene blue) of the porous starch samples crosslinked at various STMP concentrations. It can be seen from this figure that the porous starch samples having different degree of crosslinking have quite different adsorption capacity for MB. The adsorption capacity of the crosslinked porous starch at 6% STMP (ScPS-6) was the highest at all time values which can be attributed to the larger pores and highest pore density (refer to Table 1) (Yamada et al., 1995; Zhao et al., 1996). Besides, the STMP (as crosslinker) is capable of increasing the intensity of the ester linkages (crosslinking bond), which improves the stability and integrity of starch granule structure. The higher degree of crosslinking enables adsorption of higher amount of methylene blue and holds the adsorbed methylene blue molecules more tightly within the porous structure. The adsorption kinetics data also show that adsorption of methylene blue molecules occurs very rapidly within 60 min (fast adsorption stage). Then, the rate of adsorption slows down at longer times (slow adsorption stage). After 120 min, the amount of adsorbed ScPS increases very slowly with time suggesting that the adsorption process almost reaches to an equilibrium value. Furthermore, the ScPS-6 shows the best adsorption capability among these crosslinked porous starch samples which can also be contributed to its highest porosity and largest pore diameter (Table 1).

Two different kinetic models [Eqs. (4) and (5)] were used to explore the mechanism of adsorption. The first-order and the

second-order models are given by Eqs. (4) and (5), respectively (Ho & McKay, 1998).

$$\ln(Q_e - Q_t) = \ln Q_e - K_1 \times t \quad (4)$$

$$\frac{t}{Qt} = \frac{1}{K_2 \times Qe^2} + \frac{1}{Qe} \times t \quad (5)$$

where Q_e and Q_t (mg/g) are the adsorbed values of methylene blue at equilibrium and at time t, respectively. K_1 (min^{-1}) and K_2 (g/mg/min) are the equilibrium rate constants of the first order and second order equations, respectively.

The scenario of fitting of the first order kinetics model [Eq. (4)] with the experimental methylene blue adsorption kinetics data is presented in Fig. 2. The second order kinetics model was also similarly fitted with these adsorption kinetics data (not shown). The parameters obtained by fitting these two different models to experimental data are presented in Table 3. Judging from the coefficient of regression (R^2), the first order model fits the experimental data better than the second order model suggesting that the first order kinetics model better represents the adsorption kinetics of methylene blue in crosslinked porous starch samples.

The parameter K_1 represents the rate of adsorption. The higher value of this parameter indicates to a faster adsorption rate. The data presented in Table 3 shows that the ScPS-6 has the highest K_1 value indicating that this crosslinked porous starch sample possesses the best adsorption ability. The highest rate of adsorption in ScPS-6 can also be attributed to the highest porosity and pore diameter values in this sample (Table 1).

3.5. FTIR spectra of starch samples

The variation in crystal form, chain conformation and the helical structure of starch alters the absorption of infrared energy (Wu & Seib, 1990). Hence, the FTIR was used to further explore the structural organization of STMP-crosslinked porous starch samples.

The FT-IR spectra of the native starch, porous starch and STMP-crosslinked porous starch samples (ScPS) are shown in Fig. 3a. The presence of O–H is confirmed by the presence of stretching vibration at wavenumber about 3400 cm^{-1}. The peak at 1248 cm^{-1} corresponds to the O–H bending vibration. The absorption bands in the 1365–1413 cm^{-1} region are contributed by the C–H bending vibrations. The absorption band observed at 2945 cm^{-1} is due to C–H stretching. The absorption peak at 1160 cm^{-1} is due to C–O bending (Peng et al., 2011a,b; Silva-Júnior et al., 2008). As can be seen from Fig. 3a, there is no distinct difference among the vibration bands of O–H, C–H, and C–O in native starch, porous starch and different ScPS. This may be due to the fact that the basic chemical structures of the uncrosslinked porous starch, the crosslinked porous starch and the native starch are similar which has reflected in the similar absorption peaks.

However, there are some noticeable differences in the FT-IR spectrum of ScPS compared to the spectra of uncrosslinked porous starch and native starch samples. Two of the noticeable differences in these spectra are that the absorption bands in 2432–2358 cm^{-1} range have disappeared and the peak at about 1107 cm^{-1} became broader and more intense (stronger).

Interestingly, the characteristic absorption peaks inherent to P–O and P–O–C (Suflet et al., 2006) did not appear in the spectra of the crosslinked porous starch samples. This could be due to the low degree of crosslinking in these ScPS samples. However, as can be seen from Fig. 3b, the absorption peaks observed within 1000–1250 cm^{-1} of FT-IR spectrum of starch crosslinked with 8% STMP are absent in the spectra of other crosslinked porous starch samples. This means that the P–O and P–O–C absorption peaks could be observed when the degree of crosslinking with STMP was higher.

3.6. The melting point and melting enthalpy of samples

Fig. 3 (panel c and d) shows the thermograms of crosslinked starch and STMP-crosslinked porous starch. This figure also includes the thermograms of native starch and porous starch for comparison purpose. It can be seen from Fig. 3c and d that all the samples show distinct endothermic peaks between 120 °C and 160 °C. These are the melting temperatures at which the melting of the micro-crystallites of this particular starch takes place.

The peak melting point temperature of the crosslinked starch increased with the increase in the degree of crosslinking up to 6% of STMP. The peak melting temperature of the starch crosslinked with 8% STMP was lower than the starch which was crosslinked with 6% STMP. This observation indicates that the application of STMP as a crosslinker can improve the stability and integrality of native starch up to 6% of STMP, which increases the difficulty of starch melting. However, it appears that when the concentration of crosslinker or degree of crosslinking increases beyond certain value (8% STMP in this case) it increases the inhomogeneity in starch and lowers the melting point.

The thermograms of crosslinked porous starch samples are distinctly different compared to those of native starch and the porous starch in terms of peak temperature and enthalpy (ΔH). The porous starch has higher melting temperature than that of native starch. This is because starch samples hydrolyzed by enzyme possess relatively higher percentage of crystallinity, which leads to greater packing in the granules. This denser packing impedes both the heat and mass transfer which results into higher melting temperature.

The crosslinked porous starch samples showed higher melting temperature than the native starch. Among the crosslinked porous starch samples, the peak melting temperature showed decreasing trend with increase in the degree of crosslinking. The melting enthalpy (ΔH) on the other hand increased with the increase in the crosslinking degree. This may be due to the fact that the crosslinking reaction increases the average molecular mass, improves the strength of chemical bonds involved in intermolecular crosslinking. All of these factors make the starch granules stronger and favor the increase in melting enthalpy. All of these observations indicate that the crosslinked porous starch possesses better thermal stability compared to the native starch.

3.7. X-ray diffraction (XRD) patterns of starch samples

The XRD patterns of native starch, uncrosslinked porous starch and STMP-crosslinked porous starch samples are presented in Fig. 4a. Each X-ray diffractogram except for that of the native starch is vertically shifted to avoid overlapping. As can be seen from this figure, the native starch shows a typical A-type crystalline pattern (strong diffraction peaks (2θ) at about 14.8° and 22.7°) which is characteristic of cereal starch. The A-type crystalline pattern also contains an unresolved doublet at 16.9° and 17.8° (2θ) and a small diffraction peak at about 19.8° (2θ) (Whittam, Noel, & Ring, 1990). The porous starch also showed similar A-type crystalline pattern with higher intensities and sharper peaks which indicates that the enzymatic hydrolysis has not altered the physical structure of the starch (Wu, Du, Ge, & Lv, 2011). This observation is consistent with earlier study by Gallant, Mercier, and Guilbot (1972) who mentioned that the amylolysis primarily occurs in the amorphous region of the starch granules.

However, the diffraction patterns of the crosslinked porous starch samples are distinctly different compared to those of native starch and uncrosslinked porous starch samples. As can be seen from Fig. 4a, the coupled diffraction peaks at 16.9° and 17.8° (2θ) gradually started to merge into a single peak with the increase in the crosslinking degree. The diffraction peaks of the differently crosslinked porous starch samples appear at different locations.

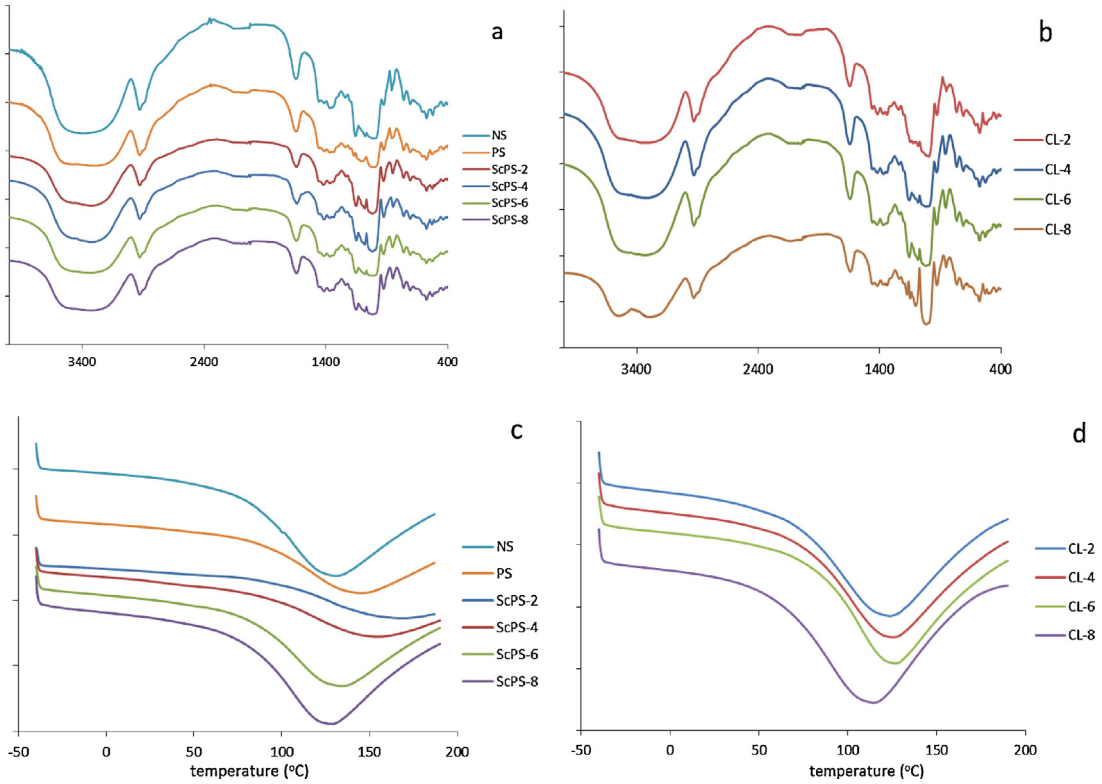

Fig. 3. The FTIR spectra and thermograms of native starch (NS), porous but uncrosslinked starch (PS), crosslinked starch (CL) and crosslinked porous starch (ScPS) samples.

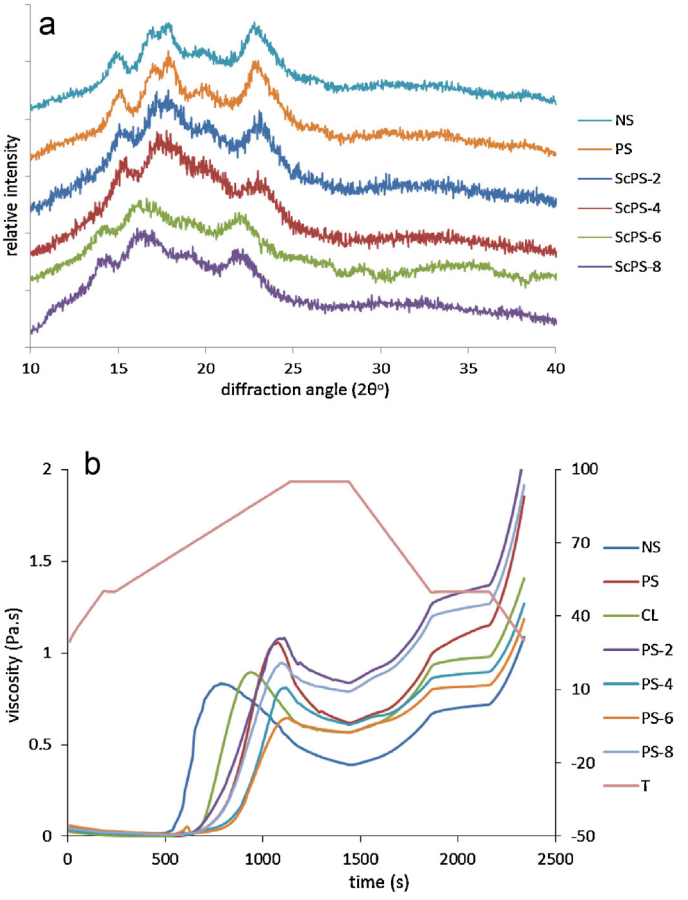

Fig. 4. X-ray diffractograms and Viscosity of native starch (NS), porous but uncrosslinked starch (PS) and crosslinked porous starch (ScPS) samples.

Besides, a diffraction peak at about 19.8° (2θ) almost disappeared in ScPS-6. The intensity of diffraction in crosslinked porous starch samples decreased quite remarkably compared to the intensity of uncrosslinked porous starch. This may be due to the fact that the crosslinking reaction between the STMP and starch molecules mainly occurs in the crystalline region of the starch granules.

3.8. Viscometric properties

The steady shear viscosity versus temperature profiles of native starch, uncrosslinked porous starch, and STMP-crosslinked porous starch are presented in Fig. 4b. As can be seen from this figure, the pasting temperature of the crosslinked starch samples increased with the increase in the degree of crosslinking. The increase in the pasting temperature is an indication that the crosslinking had indeed taken place within the starch granules and that the crosslinking increased the shear and thermal resistance.

As shown in Fig. 4b, the peak viscosity of crosslinked porous starch samples decreased from 1.081 Pa s to 0.6451 Pa s first and then increased to 0.9447 Pa s due to the increase in the degree of crosslinking with STMP. The ScPS-6 showed the lowest peak viscosity among these samples. The holding strength and final viscosity also showed similar trend shown by the peak viscosity.

Watcharatewinkul, Uttapap, Puttanlek, and Rungsardthong (2010) explained that an increase in breakdown value is an indication of breaking down of fragile starch granules. The lower breakdown viscosity values indicate better thermal stability (Saartrat, Puttanlek, Rungsardthong, & Uttapap, 2005; Chuenkamol, Puttanlek, Rungsardthong, & Uttapap, 2000). It can be observed from Table 4 that the breakdown values show clear distinction between the native starch, uncrosslinked porous starch, crosslinked starch and crosslinked porous starches. The uncrosslinked porous starch showed the highest breakdown indicating that the thermal stability of porous starch was the poorest.

Table 3
The parameters of the two kinetic models applied to predict the adsorption of methylene blue (MB) of porous starches having different crosslinking degree.

Sample	Pseudo-first-order			Pseudo-second-order		
	Q_{e1}	K_1	R_1^2	Q_{e2}	K_2	R_2^2
ScPS-2	$0.654 \pm 0.009^{a,b}$	2.185 ± 0.113^{b}	0.996	0.738 ± 0.030^{b}	3.486 ± 0.675^{c}	0.978
ScPS-4	0.758 ± 0.07^{b}	$1.996 \pm 0.067^{a,b}$	0.998	0.865 ± 0.028^{c}	2.666 ± 0.415^{a}	0.987
ScPS-6	0.814 ± 0.016^{c}	2.354 ± 0.173^{c}	0.991	0.915 ± 0.042^{d}	3.034 ± 0.688^{b}	0.970
ScPS-8	0.590 ± 0.012^{a}	1.907 ± 0.145^{a}	0.992	0.677 ± 0.034^{a}	3.182 ± 0.753^{b}	0.972

ScPS-2, 4, 6, and 8 denote 2%, 4%, 6% and 8% of crosslinking in porous starch samples.
Values represent the mean ± standard deviation of triplicate tests.
Values in a column with different superscripts were significantly different ($p < 0.05$).

Table 4
The characterstic viscometric parameters of native starch (NS), uncrosslinked porous starch (PS), crosslinked starch (CL) and crosslinked porous starch (ScPS) samples.

Sample	Parameter				
	Peak viscosity	Holding strength	Breakdown	Final viscosity	Setback
NS	0.8119	0.4005	0.4114	0.7185	0.3180
PS	1.056	0.6192	0.4368	1.150	0.5308
CL	0.8950	0.5672	0.3278	0.9785	0.4113
ScPS-2	1.0810	0.8368	0.2442	1.3690	0.5322
ScPS-4	0.8097	0.6094	0.2003	0.8961	0.2867
ScPS-6	0.6451	0.5658	0.0793	0.8231	0.2573
ScPS-8	0.9447	0.7891	0.1556	1.2670	0.4779

ScPS-2, 4, 6, and 8 denote 2%, 4%, 6% and 8% of crosslinking in porous starch samples.

This is because the uncrosslinked porous starch had the largest pores and highest pore density due to enzymatic hydrolysis. The largest pore size and the highest pore density reduced the structural stability of starch granules which was reflected in the very high breakdown value. The native starch displayed larger breakdown value than that of crosslinked starch. This better thermal and shear stability (compared to native starch) of the crosslinked starch is due to the increase in the thermal and shear resistance accorded by the STMP crosslinking. The breakdown viscosity value of ScPS-6 was 0.0793 Pa s which was the lowest among all the starch samples. This indicates that this starch sample possess excellent stability against heat and shear.

It has to be noted that although the crosslinked starch granules were stronger than the native starch granules, they were not strong enough to withstand the heat and shear during the holding period. Accordingly, vast majority of crosslinked granules were broken and interactions among the dispersed starch molecules resulted into increase in paste viscosity when the dispersions were cooled.

4. Conclusions

Corn starch was crosslinked with STMP (2%, 4%, 6% and 8%, (w/w) STMP) and subsequently partially hydrolyzed by using combination of two enzymes (alpha amylase and glucoamylase). The morphology, porosity, swelling properties, adsorption kinetics, crystallinity, thermal and viscometric properties of these crosslinked porous starch samples were determined and analyzed. The native starch and the starch which was crosslinked but not subjected to enzymatic hydrolyzed were also characterized for comparison purpose.

The porous starch crosslinked with 4% STMP showed quite different morphology compared with other crosslinked porous starch samples. The size of pores in the ScPS-4 was the smallest and the number of pores in this sample was the highest. Both the porosity and the pore diameters of the crosslinked and hydrolyzed samples increased significantly compared to those of the native starch. The porosity and pore diameter values of the ScPS-6 were the highest among all the samples. The swelling power of crosslinked porous starch was lower than that of uncrosslinked porous starch but higher than that of native starch. The uncrosslinked porous starch granules had larger pore size and higher pore density which enabled it to hold more water and, hence, increase the swelling power. The crosslinking with STMP increased the integrity of starch granules which resulted into lower swelling power.

The first order kinetic model was found to fit the experiment adsorption kinetics data of methylene blue in crosslinked porous starch well ($R^2 > 0.99$, average error = 6.03%).

The crosslinked porous starch produced by crosslinking with 6% (w/w) STMP was found to have the best resistance against effect of heat and shear. Thus, the porous starch crosslinked with 6% (w/w) STMP can find increased application in food and other industries where starch with higher shear and thermal resistance is desired.

Acknowledgments

This research was supported by High Technology Research and Development Program of China (2011AA100802), National Natural Science Foundation of China (31000813), Science and Technology Support Project of China (2013BAD10B03), and Beijing Municipal Science and Technology Commission Project (Z121100001312010, D12110003112002), Commonweal Guild Agricultural Scientific Research Program of China (201003077), and Chinese Universities Scientific Fund (2012YJ092, 2012QJ009, 2013YJ007).

References

Acquarone, V. M., & Rao, M. A. (2003). Influence of sucrose on the rheology and granule size of cross-linked waxy maize starch dispersions heated at two temperatures. *Carbohydate Polymers*, *51*(4), 451–458.
Atyabi, F., Manoochehri, S., Moghadam, S. H., & Dinarvand, R. (2006). Cross-linked starch microspheres: Effect of cross-linking condition on the microsphere characteristics. *Archives of Pharmacal Research*, *29*(12), 1179–1786.
Chang, P. R., Yu, J. G., & Ma, X. F. (2011). Preparation of porous starch and its use as a structure-directing agent for production of porous zinc oxide. *Carbohydrate Polymers*, *83*(2), 1016–1019.
Chen, C. L., Zhang, B. S., & Chen, F. O. (2011). A novel method for calculating starch crystallinity. *Journal of Food Science*, *32*(9), 68–70 [in Chinese].
Chen, G., & Zhang, B. (2012). Hydrolysis of granular corn starch with controlled pore size. *Journal of Cereal Science*, *56*(2), 316–320.
Chen, Y. S., Huang, S. R., Tang, Z. F., Chen, X. W., & Zhang, Z. F. (2011). Structural changes of cassava starch granules hydrolyzed by a mixture of α-amylase and glucoamylase. *Carbohydrate Polymers*, *85*(1), 272–275.
Chuenkamol, B., Puttanlek, C., Rungsardthong, V., & Uttapap, D. (2000). Characterization of low-substituted hydroxypropylated *Canna* starch. *Food Hydrocolloids*, *21*, 1123–1132.

De Miguel, I., Rieumajou, V., & Betbeder, D. (1999). New methods to determine the extent of reaction of epichlorohydrin with maltodextrins. *Carbohydrate Research*, *319*(1-4), 17–23.
Gallant, D., Mercier, C., & Guilbot, A. (1972). Electron microscopy of starch granules modified by bacterial alpha-amylases. *Cereal Chemistry*, *49*(3), 354–365.
Hamdi, G., Ponchel, G., & Duchêne, D. (1998). An original method for studying in vitro the enzymatic degradation of cross-linked starch microspheres. *Journal of Controlled Release*, *55*(2-3), 193–201.
Han, J. A., & BeMiller, J. N. (2008). Effects of protein on crosslinking of normal maize, waxy maize, and potato starches. *Carbohydrate Polymers*, *73*(4), 532–540.
Hermansson, A. M., & Svegmark, K. (1996). Developments in the understanding of starch functionality. *Trends in Food Science and Technology*, *7*(11), 345–353.
Hirsch, J. B., & Kokini, J. L. (2002). Understanding the mechanism of cross-linking agents (POCl3, STMP, and EPI) through swelling behavior and pasting properties of cross-linked waxy maize starches. *Cereal Chemistry*, *79*(1), 102–107.
Ho, Y. S., & McKay, G. (1998). Sorption of dye from aqueous solution by peat. *Chemical Engineering Journal*, *70*(2), 115–124.
Jobling, S. (2004). Improving starch for food and industrial applications. *Current Opinion in Plant Biology*, *7*(2), 210–218.
Kerr, R. W., & Cleveland, F. C., Jr. (1962). *Thickening agent and method of making the same. U.S. patent 3,021,222*.
Lee, J. S., Kumar, R. N., Rozman, H. D., & Azemi, B. M. N. (2005). Pasting, swelling and solubility properties of UV initiated starch-graft-poly (AA). *Food Chemistry*, *91*(2), 203–211.
Lee, K. Y., Rowley, J. A., Eiselt, P., Moy, E. M., Bouhadir, K. H., & Mooney, D. J. (2000). Controlling mechanical and swelling properties of alginate hydrogels independently by cross-linker type and cross-linking density. *Macromolecules*, *3*, 4291–4294.
Li, B. Z., Wang, L. J., Li, D., Chiu, Y. L., Zhang, Z. J., Shi, J., Chen, X. D., & Mao, Z. H. (2009). Physical properties and loading capacity of starch-based microparticles rosslinked with trisodium trimetaphosphate. *Journal of Food Engineering*, *92*(3), 255–260.
Lin, W., Yu, D., & Yang, M. (2005). pH-sensitive polyelectrolyte complex gel microspheres composed of chitosan/sodium tripolyphosphate/dextran sulfate: Swelling kinetics and drug delivery properties. *Colloids and Surfaces B: Biointerfaces*, *44*(2-3), 143–151.
Liu, Y. W. (2001). *Production and further processing of starch*. China Light Industry Press [in Chinese].
Loacutepez, O. V., Zaritzky, N. E., & Garciacutea, M. A. (2010). Physicochemical characterization of chemically modified corn starches related to rheological behavior, retrogradation and film forming capacity. *Journal of Food Engineering*, *100*(1), 160–168.
Mao, G. J., Wang, P., Meng, X. S., Zhang, X., & Zheng, T. (2006). Crosslinking of corn starch with sodium trimetaphosphate in solid state by microwave irradiation. *Journal of Applied Polymer Science*, *102*(6), 5854–5860.
O'Brien, S., & Wang, Y. J. (2008). Susceptibility of annealed starches to hydrolysis by α-amylase and glucoamylase. *Carbohydrate Polymers*, *72*(4), 597–607.
Peng, H. L., Xiong, H., Wang, S. Q., Li, J. H., Chen, L. X., & Zhao, Q. (2011a). Soluble starch-based biodegradable and microporous microspheres as potential adsorbent for stabilization and controlled release of coix seed oil. *European Food Research Technology*, *232*, 693–702.
Peng, H. L., Xiong, H., Wang, S. Q., Li, J. H., Chen, L. X., & Zhao, Q. (2011b). Soluble starch-based biodegradable and microporous microspheres as potential adsorbent for stabilization and controlled release of coix seed oil. *European Food Research Technology*, *232*(4), 693–702.
Qian, D., Chang, P. R., & Ma, X. (2011). Preparation of controllable porous starch with different starch concentrations by the single or dual freezing process. *Carbohydrate Polymers*, *86*(3), 1181–1196.
Raina, C. S., Singh, S., Bawa, A. S., & Saxena, D. C. (2007). A comparative study of Indian rice starches using different modification model solutions. *Food Science and Technology*, *40*(5), 885–892.
Saartrat, S., Puttanlek, C., Rungsardthong, V., & Uttapap, D. (2005). Paste and gel properties of low-substituted acetylated canna starches. *Carbohydrate Polymers*, *61*, 211–221.
Silva-Júnior, A. A., Scarpa, M. V., Pestana, K. C., Mercuri, L. P., de Matos, J. R., & de Oliveira, A. G. (2008). Thermal analysis of biodegradable microparticles containing ciprofloxacin hydrochloride obtained by spray drying technique. *Thermochimica Acta*, *467*(1-2), 91–98.
Singh, J., Kaur, L., & McCarthy, O. J. (2007). Factors influencing the physico-chemical morphological, thermal and rheological properties of some chemically modified starches for food applications - A review. *Food Hydrocolloids*, *21*(1), 1–22.
Suflet, D. M., Chitanu, G. C., & Popa, V. (2006). *I. Phosphorylation of polysaccharides: New results on synthesis and characterisation of phosphorylated cellulose. Reactive and Functional Polymers*, *66*(11), 1240–1249.
Svegmark, K., & Hermansson, A. M. (1993). Microstructure and rheological properties of composites of potato starch granules and amylose: A comparison of observed and predicted structure. *Food Structure*, *12*(2), 181–193.
Szabo-Revesz, P., Szepes, A., Ulrich, J., Farkas, Z., & Kovacs, J. (2007). Freeze casting technique in the development of solid drug delivery systems. *Chemical Engineering and Processing*, *46*(3), 230–238.
Uthumporn, U., Zaidul, I. S. M., & Karim, A. A. (2010). Hydrolysis of granular starch at sub-gelatinization temperature using a mixture of amylolytic enzymes. *Food and Bioproducts Processing*, *88*(1), 47–54.
Wang, Y., & Wang, L. (2003). Physicochemical properties of common and waxy corn starches oxidized by different levels of sodium hypochlorite. *Carbohydrate Polymers*, *52*(3), 207–217.
Watcharatewinkul, Y., Uttapap, D., Puttanlek, C., & Rungsardthong, V. (2010). Enzyme digestibility and acid/shear stability of heat-moisture treated canna starch. *Starch/Stärke*, *62*(3-4), 205–216.
Wattanchant, S., Muhammad, K., Hashim, D., & Rahman, R. A. (2003). Effect of crosslinking reagents and hydroxypropylation levels on dual-modified sago starch properties. *Food Chemistry*, *80*(4), 463–471.
Whistler, R. L. (1991). *U.S. Pat. 485082. Microporous granule starch matrix composition.*
Whittam, M. A., Noel, T. R., & Ring, S. G. (1990). Melting behaviour of A- and B-type crystalline starch. *International Journal of Biological Macromolecules*, *12*(6), 359–362.
Wongsagonsup, R., Shobsngob, S., Oonkhanond, B., & Varavinit, S. (2005). Zeta potential and pasting properties of phosphorylated or crosslinked rice starches. *Starch/Stärke*, *57*(1), 32–37.
Woo, K. S., & Seib, P. A. (1997). Cross-linking of wheat starch and hydroxypropylated wheat starch in alkaline slurry with sodium trimetaphosphate. *Carbohydrate Polymers*, *33*(4), 263–271.
Wu, Y., Du, X., Ge, H., & Lv, Z. (2011). Preparation of microporous starch by glucoamylase and ultrasound. *Starch/Stärke*, *63*(4), 217–225.
Wu, Y., & Seib, P. A. (1990). Acetylated and hydroxypropylated distarch phosphates from waxy barley: Paste properties and freeze-thaw stability. *Cereal Chemistry*, *67*(2), 202–208.
Wurzburg, O. B. (1986). *Modified starches: Properties and uses*. Boca Raton, FL: CRC Press.
Yamada, T., Hisamatsu, M., Teranishi, K., Katsuro, K., Hasegawa, N., & hayashi, M. (1995). Components of the porous maize starch granule prepared by amylase treatment. *Starch/Stärke*, *47*(9), 358–361.
Yan, H., & Zhengbiao, G. U. (2012). Morphology of modified starches prepared by different methods. *Food Research International*, *43*(3), 767–772.
Yook, C., Pek, U. H., & Park, K. H. (1993). Gelatinization and retrogradation characteristics of hydroxypropylated cross-linked rices. *Journal of Food Science*, *58*(2), 405–407.
Yu, J., & Liu, J. (1994). Effects of suspension crosslinking reacting conditions on the size of starch microspheres. *Starch/Stäke*, *46*(7), 252–255.
Zhang, B., Cui, D., Liu, M., Gong, H., Huang, Y., & Han, F. (2012). Corn porous starch: Preparation, characterization and adsorption property. *International Journal of Biological Macromolecules*, *50*(1), 250–256.
Zhao, J., Madson, M. A., & Whistler, R. L. (1996). Cavities in porous corn starch provide a large storage space. *Cereal Chemistry*, *73*(3), 379–380.
Zhou, Y. G., Li, D., Wang, L. J., Özkan, N., Chen, X. D., & Mao, Z. H. (2006). Influences of microemulsion cross-linking reaction and ball-milling on particle size characteristics of potato and maize starches. *International Journal of Food Engineering*, *2*(4.). Article 6.